Electronic Supplementary Material (ESI) for Dalton Transactions.

Supporting Information for

One Dimensional Metal Dithiolene (M = Ni, Fe, Zn) Coordination Polymers for the Hydrogen Evolution Reaction

Courtney A. Downes and Smaranda C. Marinescu*

Department of Chemistry, University of Southern California, Los Angeles, CA, 90089, USA

*Email: smarines@usc.edu

Physical Methods

FT-IR spectra were acquired using a Bruker Vertex 80v spectrometer. Samples (2 mg) for analysis were mixed into a KBr (100 mg) matrix and pressed into pellets.

Raman spectra were collected on a Horiba Raman Microscope using films of **4**, **5**, and benzene-1,2,4,5-tetrathiol on glass microscope slides.

UV-Vis absorption spectra were measured with a Perkin Elmer Lamba 950 equipped with a 150 mm integrating sphere. The coordination polymers **4**–**6** were each deposited onto a quartz microscope slide and washed with water, methanol, and ethyl acetate before analysis.

Inductively coupled plasma optical emission spectroscopy (ICP-OES) measurements were performed using a Thermo Scientific iCAP 7000 ICP-OES.
XPS data were collected using a Kratos AXIS Ultra instrument. The monochromatic X-ray source was the Al K α line at 1486.6 eV, directed at 35° to the sample surface (55° off normal). Emitted photoelectrons were collected at an angle of 35° with respect to the sample surface (55° off normal) by a hemispherical analyzer. The angle between the electron collection lense and X-ray source is 71°. Low-resolution survey spectra were acquired between binding energies of 1–1200 eV. Higher-resolution detailed scans, with a resolution of ~0.1 eV, were collected on individual XPS lines of interest. The sample chamber was maintained at $< 2 \times 10^{-9}$ Torr. The XPS data were analyzed using the CasaXPS software.

Scanning electron microscopy (SEM) was performed on a JEOL JSM 7001F scanning electron microscope.

The aqueous solutions used in the electrochemical experiments have been prepared as follows. For the pH 1.3 solution, 0.534 mL of 18.7 M H_2SO_4 were added to water (200 mL). For the pH 2.6 solution, citric acid (3.458 g) and Na_2HPO_4 (1.505 g) were dissolved in water (200 mL). For the pH 4.4 solution, NaOAc (1.605 g) was dissolved in water (200 mL). Acetic acid (1.2 mL) was added to reach the desired pH. For the pH 7.1 solution, NaH_2PO_4 (0.468 g) and Na_2HPO_4 (1.637 g) were dissolved in water (100 mL). For the pH 10.0 solution, $NaHCO_3$ (0.339 g) and

Na_2CO_3 (0.632 g) were dissolved in water (100 mL). The pHs of the solutions were measured with a benchtop Mettler Toledo pH meter. All solutions were degassed and purged with nitrogen.

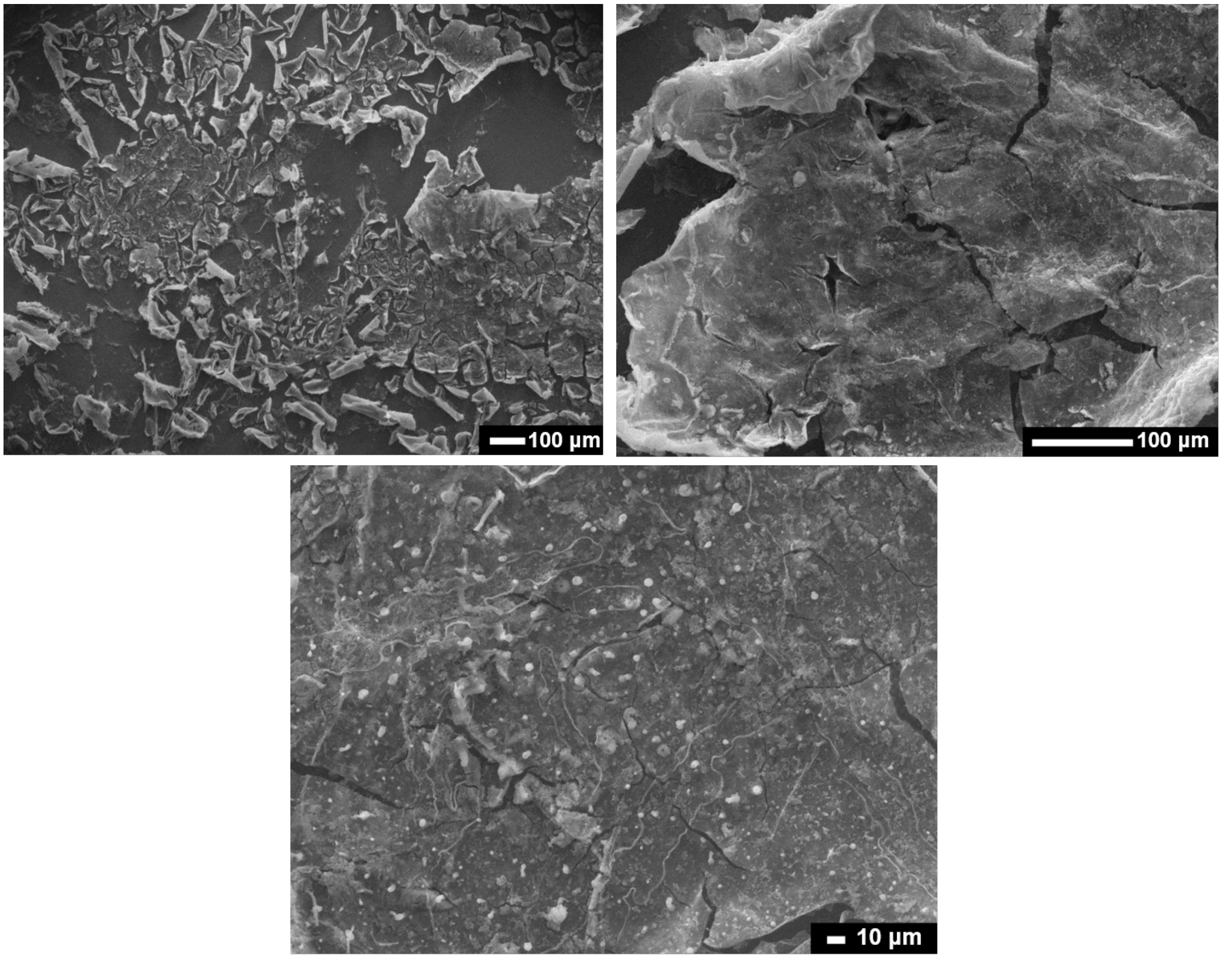

Figure S1. Top-down scanning electron microscopy images of **4.**

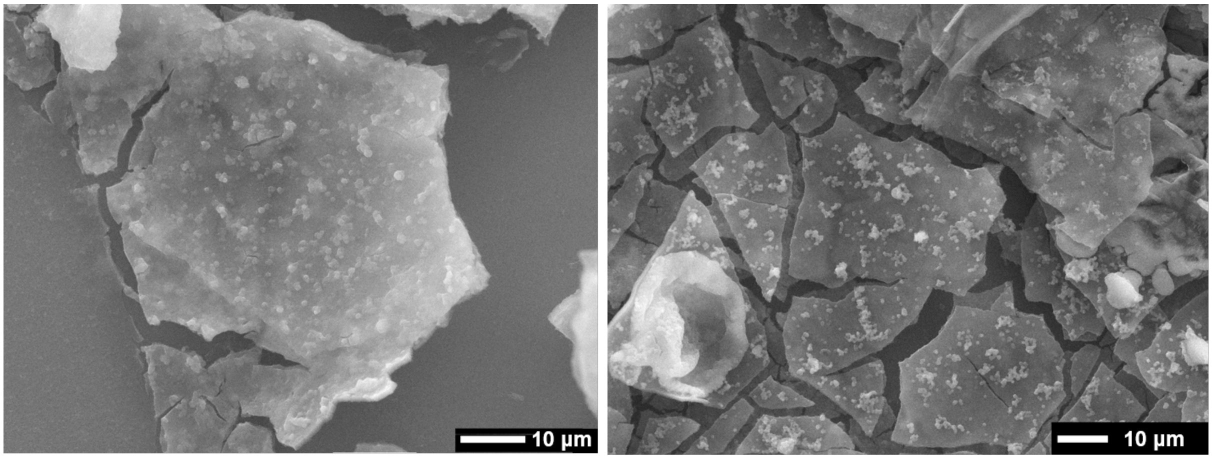

Figure S2. Top-down scanning electron microscopy image of **5**.

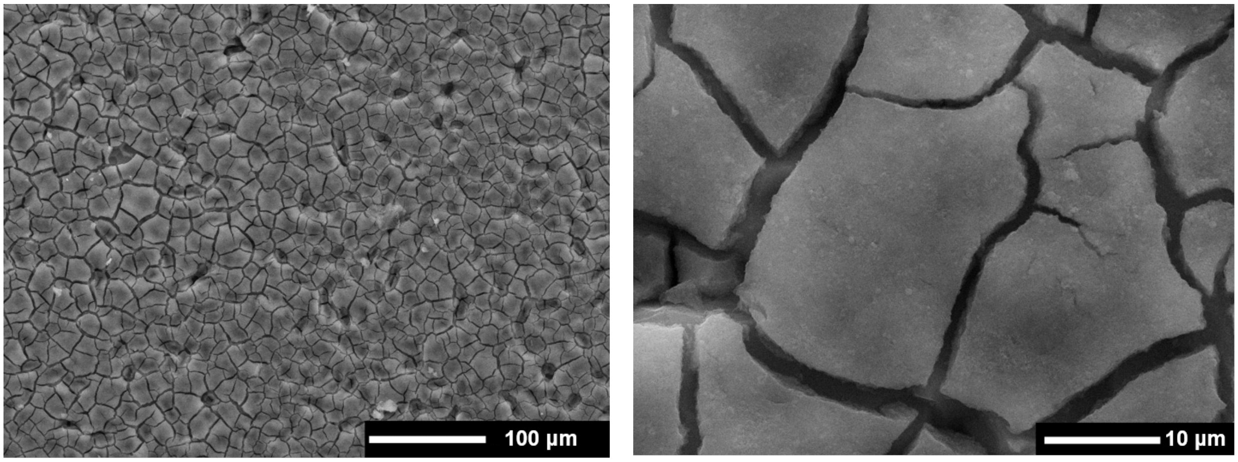

Figure S3. Top-down scanning electron microscopy images of **6**.

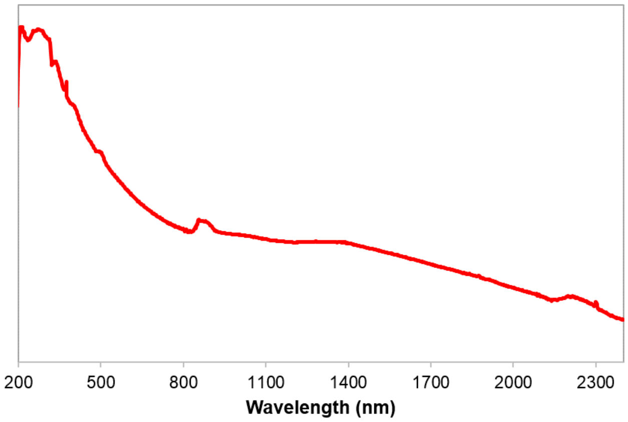

Figure S4. UV-Vis spectrum of **4** on a quartz microscope slide.

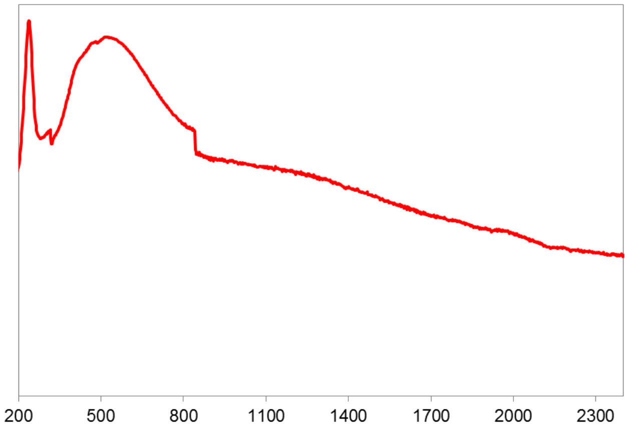

Figure S5. UV-Vis spectrum of **5** on a quartz microscope slide.

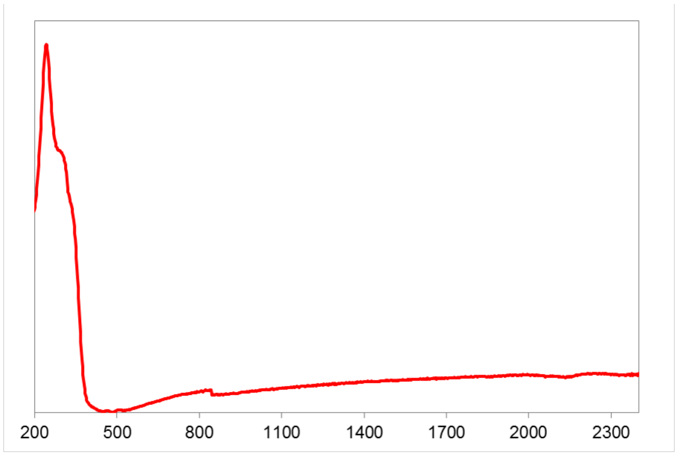

Figure S6. UV-Vis spectrum of **6** on a quartz microscope slide.

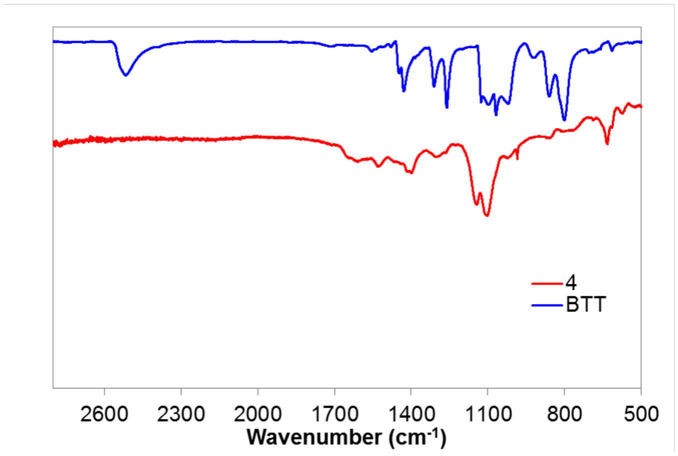

Figure S7. FTIR spectra of **4** (red) and benzene-1,2,4,5-tetrathiol (BTT) (blue).

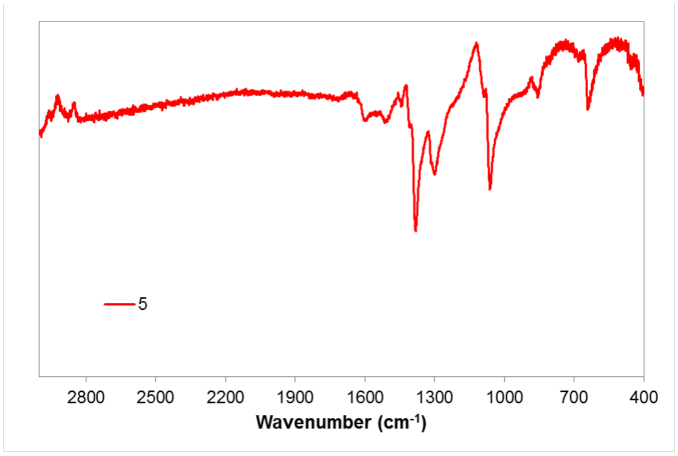

Figure S8. FTIR spectra of **5**.

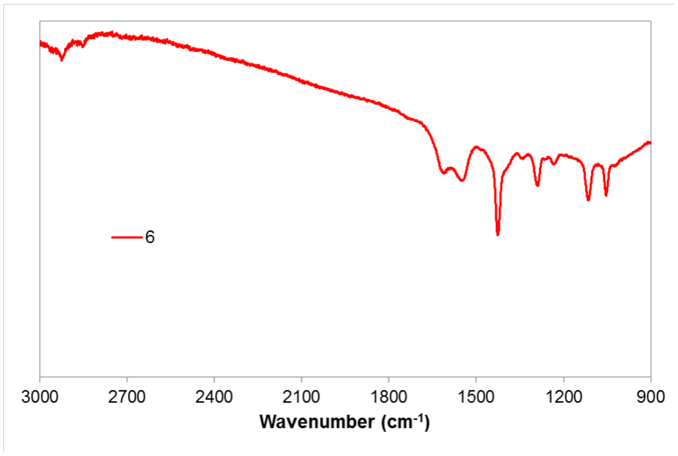

Figure S9. FTIR spectra of **6**.

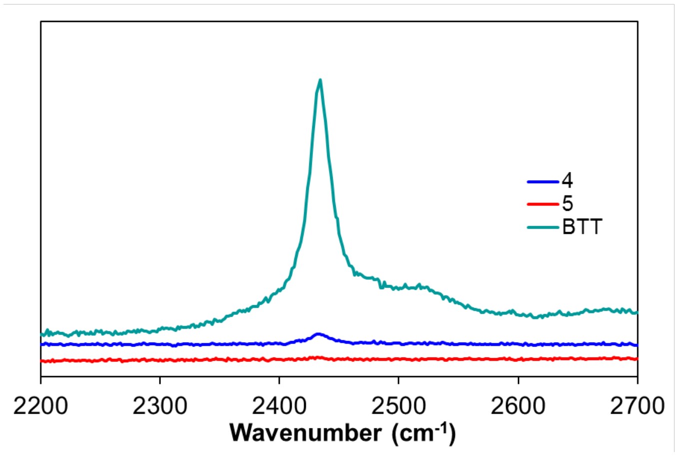

Figure S10. Raman spectroscopy of **4** (blue), **5** (red), and benzene-1,2,4,5-tetrathiol (BTT, cyan).

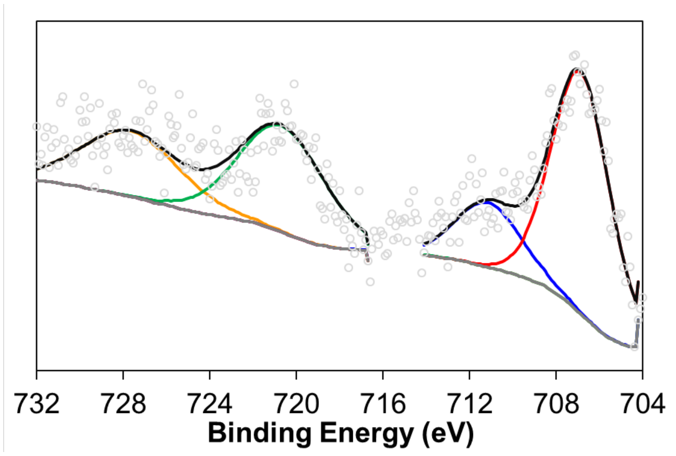

Figure S11. XPS of Fe 2p core level of $[Fe(bdt)_2]^-$ (where bdt = 1,2-benzenedithiolate).

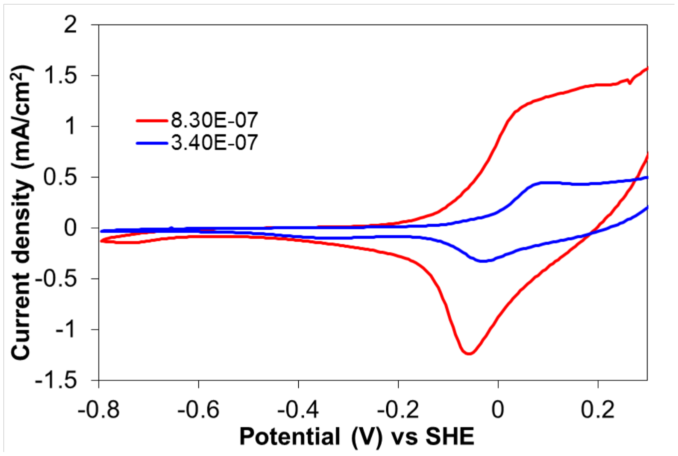

Figure S12. Polarization curves of **5** at differing catalyst loadings ($8.3(8)\times10^{-7}$ mol_{Fe}/cm^2 (red) and $3.4(3)\times10^{-7}$ mol_{Fe}/cm^2 (blue)) in 0.1 M $NaClO_4$ aqueous solutions at pH 10.0; scan rate: 20 mV/s.

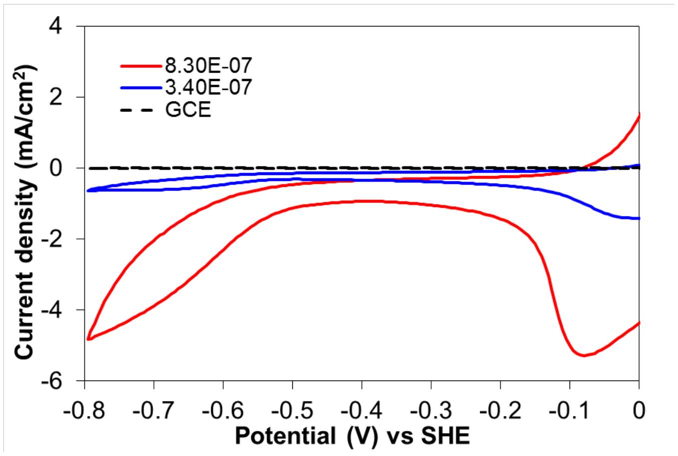

Figure S13. Polarization curves of **5** at differing catalyst loadings ($8.3(8)\times10^{-7}$ mol_{Fe}/cm^2 (red) and $3.4(3)\times10^{-7}$ mol_{Fe}/cm^2 (blue)) and blank GCE (dashed black) measured in 0.1 M $NaClO_4$ aqueous solutions at pH 1.3; scan rate: 20 mV/s.

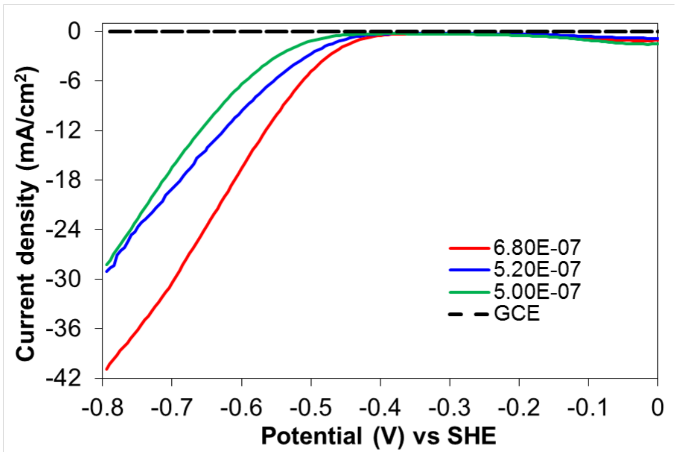

Figure S14. Polarization curves of **4** at different catalyst loadings in 0.1 M $NaClO_4$ aqueous solutions at pH 1.3 (a) $6.8(7) \times 10^{-7}$ mol_{Ni}/cm^2 (red) (b) $5.2(5) \times 10^{-7}$ mol_{Ni}/cm^2 (blue) (c) $5.0(5) \times 10^{-7}$ mol_{Ni}/cm^2 (green) (d) blank GCE (dashed black).

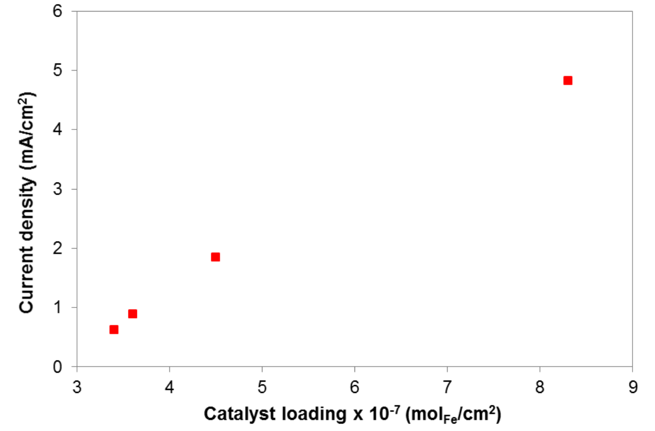

Figure S15. Current densities of **5** measured at –0.80 V vs SHE at pH 1.3 as a function of the surface catalyst concentration. The surface concentration was quantified by integrating the peak area at pH 10.0. Scan rate: 20 mV/s.

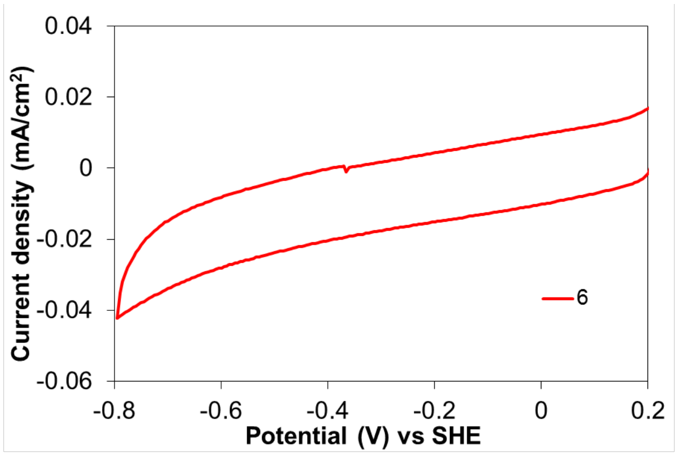

Figure S16. Polarization curve of **6** in 0.1 M $NaClO_4$ aqueous solution at pH 10.0; scan rate: 20 mV/s.

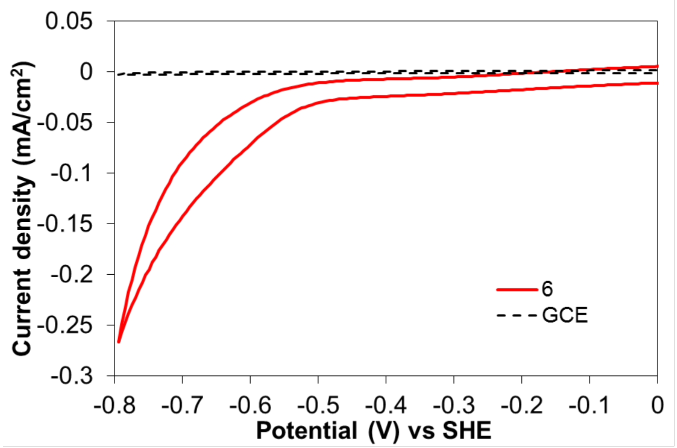

Figure S17. Polarization curves of **6** (red) and blank GCE (black dashed) in 0.1 M $NaClO_4$ aqueous solutions at pH 1.3; scan rate: 20 mV/s.

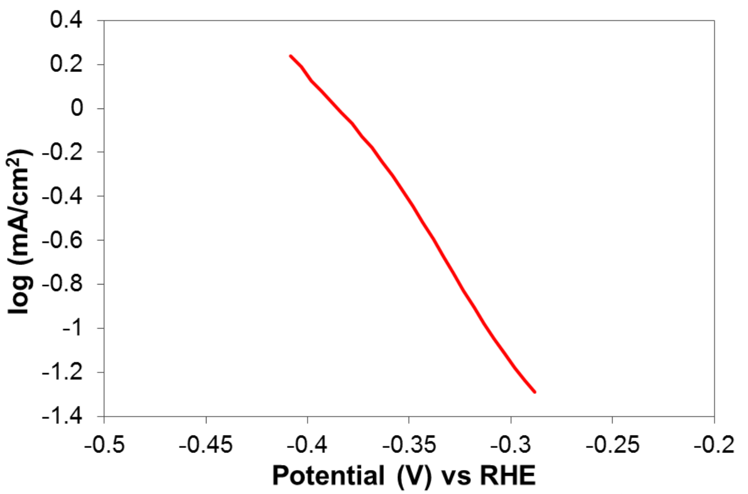

Figure S18. Tafel plot of **4** (catalyst loading: $5.6(6) \times 10^{-7}$ mol_{Ni}/cm^2) in 0.1 M $NaClO_4$ aqueous solutions at pH 2.6. Scan rate: 0.5 mV/s; Tafel slope of 76 mV/dec; exchange current density of $10^{-8.1}$ A/cm^2.

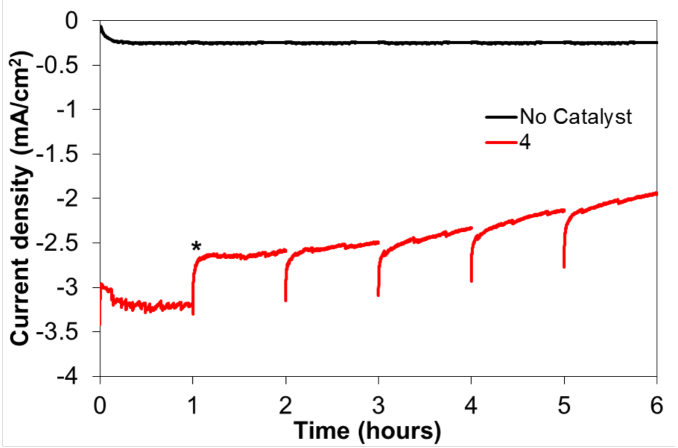

Figure S19. Controlled potential electrolysis (CPE) studies of **4** ($1.2(1) \times 10^{-7}$ mol_{Ni}/cm^2;red) and blank GCE (black) at –0.80 V vs SHE in 0.1 M $NaClO_4$ aqueous solutions at pH 1.3. The asterisk indicates the removal of 10 mL of 60 mL headspace in the working compartment of the H-cell for gas chromatography experiments. This led to a rapid change in the solution level resulting in the abrupt drop off in the current density.

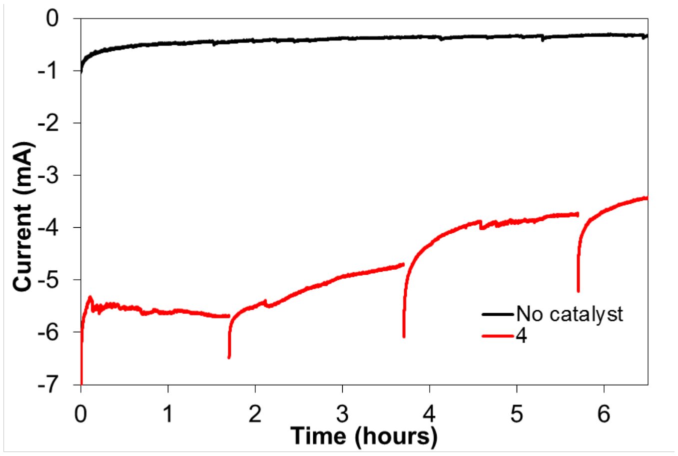

Figure S20. CPE studies of **4** ($1.4(1) \times 10^{-7}$ $\mathrm{mol_{Ni}/cm^2}$) at –0.80 V vs SHE in 0.1 M $NaClO_4$ aqueous solutions at pH 2.6 (red) and of blank GCE (black).

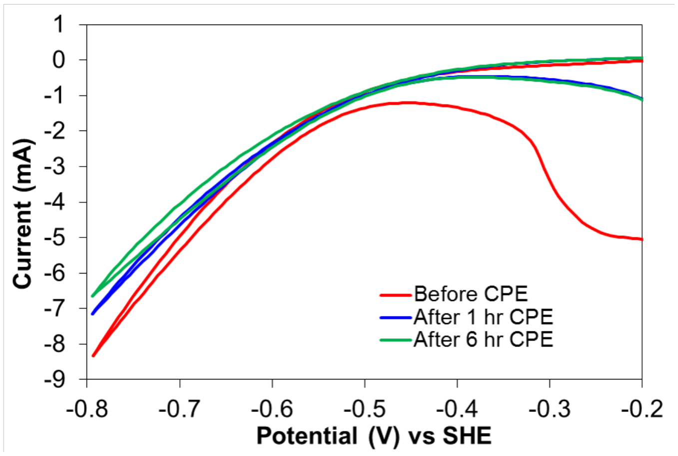

Figure S21. Polarization curves of **4** ($1.4(1) \times 10^{-7}$ $\mathrm{mol_{Ni}/cm^2}$) in 0.1 M $NaClO_4$ aqueous solutions at pH 2.6 before CPE experiment (red), after 1 hour CPE (blue), and after 6 hour CPE (green).

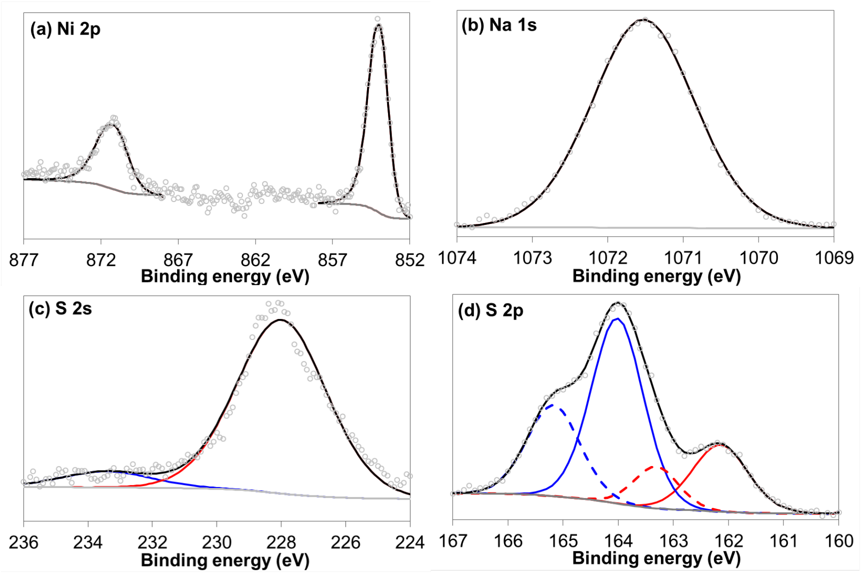

Figure S22. XPS analysis of **4** after 6 h CPE studies in 0.1 M $NaClO_4$ aqueous solutions at pH 1.3 (a) Ni 2p core level XPS spectrum; (b) Na 1s core level XPS spectrum; (c) S 2s core level XPS spectrum; (d) S 2p core level XPS spectrum.

(1) Dirk, C. W.; Cox, S. D.; Wellman, D. E.; Wudl, F. *J. Org. Chem.* **1985**, *50*, 2395–2397.

(2) (a) Xiong, Q. et. al *ACS Nano*, **2014**, *8*, 1597-10605. (b) Bonnissel-Gissinger, P.; Alnot, M.; Ehrhardt. J. J.; Behra, P. *Environ. Sci. Technol.*, **1998**, *32*, 2839-2845.